Science of the Total Environment 935 (2024) 173429

Contents lists available at ScienceDirect

Science of the Total Environment

journal homepage: www.elsevier.com/locate/scitotenv

Effect of particle density on microplastics transport in artificial and natural porous media

Wang Li [a,*], Giuseppe Brunetti [b], Anastasiia Bolshakova [a], Christine Stumpp [a]

[a] University of Natural Resources and Life Sciences, Vienna, Department of Water, Atmosphere and Environment, Institute of Soil Physics and Rural Water Management, Muthgasse 18, 1190 Vienna, Austria
[b] University of Calabria, Department of Civil Engineering, Rende, Italy

HIGHLIGHTS

- Mobility of microplastics depends on the plastic density.
- Highest mobility was found for microplastics of 1 g cm^{-3} and lowest for 1.12 g cm^{-3}.
- Similar transport behavior of microplastic was observed in gravel and glass beads.
- Retention profiles are needed for the simulation of microplastic fate.
- Model with depth-dependent blocking function well interprets all MPs' fate in the effluent.

GRAPHICAL ABSTRACT

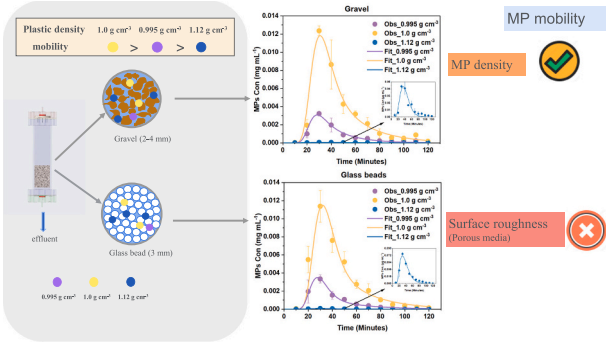

ARTICLE INFO

Editor: Thomas Kevin V

Keywords:
Microplastics
Density
Transport
Sediments
Glass beads
HYDRUS 1D

ABSTRACT

The occurrence and persistence of microplastics (MPs) in natural environments are of increasing concern. Along with this, the transport of MPs in sediments has been investigated mainly focusing on the effect of plastic size and shape, media size effect, and solution chemistry. Yet, the influence of particle density is only partially understood. Therefore, column experiments on the transport of variably buoyant MPs in saturated natural sediments and glass beads were conducted, and transport parameters were quantified using a two-site kinetic transport model with a depth-dependent blocking function (the amount of retained MPs does not decrease at a constant rate with increasing depth, the majority of MPs were retained near the column inlet). Neutral, sinking, and buoyant MPs within the same size range were selected, with stable water isotope applied as conservative tracer to explore water and MP movement in the tested sediments. The results showed that 95.5 ± 1.4% of sinking MPs remained in columns packed with gravel, followed by buoyant and neutral MPs, thus indicating that particle density does affect MP mobility. Similar recovered amounts of MPs were found in columns packed with glass beads, indicating that tested sediment types do not affect the deposition behavior of MPs. The breakthrough curves of MPs were accurately described by the selected model. However, the simulated retention profiles overestimated the observed MP amount in layers closest to the column inlet. The coupled experimental and modeled results suggest an enhanced retention of sinking MPs, while neutrally and buoyant MPs exhibit a higher mobility in comparison. Thus, neutral or buoyant MPs can potentially pose a higher contamination risk to

* Corresponding author.
E-mail address: wang.li@boku.ac.at (W. Li).

https://doi.org/10.1016/j.scitotenv.2024.173429
Received 20 March 2024; Received in revised form 7 May 2024; Accepted 19 May 2024
Available online 22 May 2024

subsurface porous media environments compared to sinking MPs. Discrepancies between observed and simulated retention profiles indicate that future model development is needed for advancing the MP deposition as affected by particle density.

1. Introduction

Microplastics (MPs), plastic sizes smaller than 5 mm (Thompson et al., 2004) have been found in soils (Hu et al., 2021; Liu et al., 2018) and groundwater bodies with different concentrations (Mintenig et al., 2019; Mu et al., 2022; Samandra et al., 2022), and they can be translocated to other environmental compartments due to water flow (Park et al., 2023) or soil invertebrates (Zhao et al., 2022a, 2022b). To assess the potential leaching risk of MPs to groundwater, it is essential to understand the transport fate and mechanism of MP. The current literature provides contrasting evidence on the migration of MPs towards deeper soil horizons, with some studies emphasizing limited downward transport due to the combined effect of sorption and blocking processes in the unsaturated zone (Fei et al., 2023; Rong et al., 2023), and others reporting detectable MPs concentrations in deep soils (Hu et al., 2021; Weber and Opp, 2020). Simultaneously, multiple studies focusing on column experiments have examined the factors influencing the MPs' mobility in porous media, specifically, plastic size (Bradford et al., 2002; Chrysikopoulos and Katzourakis, 2015; Han et al., 2022; Leij and Bradford, 2013; Li et al., 2024), shape (Ma et al., 2011; Salerno et al., 2006; Waldschläger and Schüttrumpf, 2020), polymer type (Fei et al., 2022; Ren et al., 2021), solution chemistry (Bennacer et al., 2017; Zhao et al., 2022a, 2022b), input concentration (Bradford and Bettahar, 2006; Zhang et al., 2023), and grain size (Bradford et al., 2005; Li et al., 2024). However, the impact of plastic density on MP mobility remains largely unexplored. Additionally, plastic density has been discussed as the most decisive parameter that control the terminal settling velocities, which increased with increasing particle density (Ahmadi et al., 2022). Therefore, it can be hypothesized that higher sinking rates are expected for denser MPs, resulting in fast vertical transport velocities in porous media.

Previous studies have mainly focused on comparing the transport of MPs and other denser particles. For example, experiments conducted by Sharma et al. (2008), using hydrophilic polystyrene (PS) MPs (1.05 g cm^{-3}), silica (2 g cm^{-3}), and hematite (5.26 g cm^{-3}), showed that heavier particles exhibit higher attachment coefficients compared to lighter PS MPs. Liu et al. (2019) reported flow rate and density-dependent deposition of particles, particularly, dense glass particles (2.65 g cm^{-3}) deposited more under low flow rates (20 μL min^{-1}) than under high flow rates (60 μL min^{-1}). In contrast, the deposition of light PS MPs (1.05 g cm^{-3}) increased with increasing flow rate, suggesting that high Reynolds number enhanced the blocking efficiency. It was also reported that large flow rates can increase the mobility of MPs by reducing gravitational sedimentation (Yiantsios and Karabelas, 2003). This was further confirmed by Chen and Bai (2012), who reported a strong impact of gravity under low flow velocity. Conversely, experimental data from Waldschläger and Schüttrumpf (2020) showed that density did not play a significant role in determining the maximum infiltration depth of fiber fragments in columns packed with glass beads, despite the fact that tested fibers and fragments were of different polymer types but same dimension (0.5 × 5 mm, 1–2 mm for fiber and fragment, respectively); worth emphasizing that mechanisms driving the mobility of buoyant and sinking MPs are still not clear.

Classic colloid filtration theory (CFT) has been applied to model the transport of colloids in porous media (Harvey and Garabedian, 1991; Schijven et al., 2003). The CFT model assumes a constant attachment rate of particles, resulting in monotonic retention profiles, where the amount of retained particles decreases exponentially with increasing depth (Logan et al., 1995). However, discrepancies between experimental and simulated results with CFT have been reported for MPs (Johnson et al., 2018; Tufenkji and Elimelech, 2004). Surface heterogeneity of porous media (Johnson and Elimelech, 1995), and colloid properties (Li et al., 2004) have been discussed to contribute to this deviation. Besides, particle retention profiles tend to be hyper-exponential (Li et al., 2004); in this case, the model with a blocking function was suggested to better describe the transport behavior of MPs/NPs (Bradford et al., 2002, 2003). The blocking function demonstrates that the retention of MPs is depth-dependent, and particles were retained irreversibly within porous media due to size exclusion, with the rate of particle retention decreasing with increasing migration distance (Bradford et al., 2002; Li et al., 2004). This refers to straining, a physical process, and the possibility of straining can be determined by the particle-to-grain size ratio, which shares similarities with filtration related to the retention process of particles (Bradford et al., 2006). However, the straining only occurs within the grain-grain contact region, thus involving only a small fraction of pore space (Bradford et al., 2006). Particles cannot travel through when their size exceeds the critical value. Different critical values were suggested in different studies, i.e., 0.002 defined by Bradford et al. (2003), 0.005 by Bradford et al. (2004), and 0.18 by Gerba and Keswick (1981). Thus, a model with straining was recommended to fit the transport behavior of MPs/NPs (Bradford et al., 2004). It was shown that the two-site transport model with a blocking function describes two independent deposition fates of particles, and it does not decrease exponentially with increasing migration distance. This was tested in a previous work to successfully fit the breakthrough curves and retention profiles for relatively larger MPs (> 20 μm) (Li et al., 2024). However, the two-site transport model has not been examined to simulate the transport of MPs in terms of particle density effect, thus the goodness of the current model fit still needs to be tested.

Previous findings clearly identified the need to further examine the density effects on MP transport in porous media and to test numerical models to predict the fate of MPs with different densities in the environment. Therefore, the objective of this study is to investigate, compare, and quantify the transport of MPs with different densities in porous media. To achieve the objective, observations from laboratory experiments on the mobility of different MPs in saturated artificial and natural porous media were combined with the mechanistic model HYDRUS-1D. First, a tracer solution and PE microspheres (27–35 μm) of different densities i.e., 0.995, 1.0, and 1.12 g cm^{-3}, hereafter referred to as buoyant, neutral, and sinking MPs to the water density of 1.0 g cm^{-3}, respectively - were injected into columns packed with glass beads and natural sediments. Then, tracer and MPs concentrations in the effluent, as well as MPs concentrations in the porous media (retention profile, RPs), were used to calibrate the advection-dispersion equation coupled with two-site sorption kinetics with first-order attachment-detachment coefficients and depth-dependent blocking function. Finally, experimental and modeling results were discussed to identify mechanisms regulating the migration of buoyant, neutral, and sinking MPs in artificial and natural porous media. The findings in this study will provide insights into the effect of plastic density on MP mobility in different porous media.

2. Methodology

2.1. Microplastics

Fluorescent PE microspheres (27–35 μm) of different densities (Table 1) were obtained from Cospheric LLC (Santa Barbara, CA, USA). The density of MPs and the mass of individual MP were provided by the

supplier (buoyant MPs, 0.995 cm^{-3}; neutral MP, 1.0 g cm^{-3}; sinking MPs, 1.12 g cm^{-3}). Fourier-transform infrared spectroscopy (FTIR) was applied to verify the polymer type of tested MPs (Li et al., 2024). MPs have a negative surface charge, and the zeta potential was measured with a Zetasizer (Nano-ZW, Malvern Panalytical). Tween 20 (Sigma-Aldrich) was employed to prepare well-dispersed MP suspension for uniform distribution required for injection into the column, with 2 mg MPs of each density mixed and vortexed with 2 mL 0.1% Tween 20. The same concentration and amount of surfactant to avoid MP aggregates and the difference between the set-ups related to the surfactant only in all column experiments. The presence of cationic and anionic surfactants could affect the transport behaviors of particles in porous media (Jarvie et al., 2009; Jiang et al., 2021); however, it needs to be added to avoid other aggregation. Due to the strong hydrophobicity of applied PE MPs in this work, the application of surfactant could improve the suspendability and avoid undesirable particle size effects caused by aggregation. Unlike other ionic surfactants, Tween 20 is an uncharged surfactant, which does not affect the surface charge of MPs (Jarvie et al., 2009), and it has been widely used in food, pharmaceutical, and cosmetic industries (Kralova and Sjöblom, 2009), with its occurrence in the natural environment has been reported (Olkowska et al., 2011). Therefore, MP transport in natural compartments with the presence of surfactant can be expected. Due to the challenges in representative soil sampling (Yu and Flury, 2021) and analytic methods (Bläsing and Amelung, 2018), heterogeneous MP concentration in soil has been reported (Büks and Kaupenjohann, 2020); the concentration of MPs was 0.01–55.5 mg kg^{-1} in Swiss floodplain soil (Scheurer and Bigalke, 2018), and up to 500–67,500 mg kg^{-1} in an industrial area located in Australia (Fuller and Gautam, 2016). Hence, environmentally relevant, low concentrations of MPs were applied in this work, which is 0.00125% (w:w, 12.5 mg kg^{-1}) for MPs of different densities.

2.2. Porous media

Gravel (2–4 mm) was obtained by sieving the sediments collected from a gravel pit located in Bruckmühl (Germany). Sediments were air-dried with debris removed, and then further sieved into the desired fraction without additional purification. Uniform soda-lime glass beads with a diameter of 3 mm were purchased from Avantor®.

2.3. Column experiment

Column experiments were conducted in duplicate. The protocol applied in this study is similar to what was reported in Li et al. (2024). The diagram of the experiments set up was provided in Supporting Information SI Fig. S1. Briefly, porous media were introduced into the column (inner diameter, 5 cm) to a height of 5 cm under saturated conditions, with a tube connected between the column bottom and syringe to maintain the water level above the porous media during the packing process. To avoid trapped air bubbles and layering, a stainless-steel spoon was used to mix after filling the column to an increased height of 1 cm. The porosity (0.39) was the same for all columns with different treatments. Packed columns were then equilibrated to steady-state flow conditions by pumping tap water overnight with a constant flow rate (1 mL min^{-1}).

Deuterated water was applied as a conservative tracer to characterize the hydro-dispersive properties of porous media. Two milliliters of tracer solution were pulse-injected into the column, followed by tap water pumped into the column in the downward direction for 120 min. A fraction collector equipped with 25 mL glass vials was used to collect the effluent every 3 min. A total of 40 effluent samples were collected from each column and then analyzed for δ^2H with Cavity Ring-Down Isotope Spectrophotometer (Picarro L2130-i) with a precision of ±1 ‰. Relative deuterium value (in delta) was converted to mg L^{-1} (Becker and Coplen, 2001).

After the tracer experiments were completed, MP suspension was added to the column surface with a glass pipette, and the effluent was collected every 10 min. Effluent samples were filtrated directly with regenerated cellulose filters (47 mm diameter, 0.45 μm pore size) by a vacuum pump. The packed column was then sacrificed by transferring every 1 cm porous media into 400 mL beakers, to obtain the spatial distribution of MPs retained in the porous materials. Density separation (saturated sodium chloride NaCl solution) was selected for extracting MPs from gravel and glass beads, and the collected supernatant was then filtrated. Considering the detection limits of other instruments (e.g. UV–Vis spectrophotometer, particle counter) and low input concentration applied in this work, all filtrated samples were quantified with confocal microscopy (SP8, Leica). The number of MP per sample was obtained from microscopy scanning and ImageJ software counting. Fluorescent MPs of different densities with different dyes, hence it can be differentiated by applying different fluorescent cubes during microscopy scanning, as shown in SI Fig. S2. Based on the table (particle mass to particle number calculation) provided by the supplier, particle number concentration (particle mL^{-1}) was converted to mass concentration (mg mL^{-1}) with the sample volume known. This could ensure precise detection of MP concentration though under low concentration (SI Fig. S2).

Table 1
Properties of microplastics and sediments packed into the columns (bulk density, 1.625 g cm^{-3}; flow rate 0.05 cm min^{-1}; saturated water content, 0.39 and summary of mass balance information in all column experiments. (d_{50} = median grain size of porous media, α_L = the dispersivity from conservative tracer experiment, M_E = recovered microplastics mass from effluent, M_S = recovered microplastics mass from porous media, M_T = total recovered microplastics mass).

Experiment set	Porous media	d_{50}	Particle size	Particle density	Zeta potential	MPs Input concentration			M_E	M_S	M_T
						Mass	Concentration	Particle number			
		(mm)	(μm)	(g cm^{-3})	(mV)	(mg)	mg mL^{-1}	–	%	%	%
Density impact	Gravel	3	27–35	0.995	−19.3	2	1	149,535	6.0 ± 1.10	86.34 ± 0.74	92.33 ± 1.84
			27–32	1	−10.3	2	1	148,787	22.89 ± 4.34	72.94 ± 2.94	95.82 ± 7.28
			27–32	1.12	−9.07	2	1	132,846	0.09 ± 0.012	95.51 ± 1.43	95.60 ± 1.44
Density impact	Glass beads	3	27–35	0.995	−19.3	2	1	149,535	5.1 ± 0.47	86.91 ± 0.14	92.01 ± 0.61
			27–32	1	−10.3	2	1	148,787	20.09 ± 0.31	76.38 ± 0.76	96.47 ± 1.07
			27–32	1.12	−9.07	2	1	132,846	0.12 ± 0.006	93.86 ± 2.8	93.99 ± 2.81

2.4. Modeling theory

2.4.1. Tracer transport

The tracer transport was described by the one-dimensional (1D) advection and dispersion model (ADE):

$$\frac{\partial C}{\partial t} = -\nu\frac{\partial C}{\partial x} + D_L\frac{\partial^2 C}{\partial^2 x} \tag{1}$$

where C is the tracer concentration in the liquid phase [ML^{-3}], t is time [T], v is the pore water velocity [LT^{-1}], $v = q/n$ (q is darcy velocity, $q = Q/A$ (A is the cross area), n is the effective porosity), x is the flow length [L], which is 5 cm in this work, and D_L is the longitudinal dispersion coefficient [L^2T^{-1}], defined as follows:

$$D_L = \alpha_L v \tag{2}$$

where α_L is the dispersivity [L]. The effect of the molecular diffusion is considered negligible (Gramling et al., 2002). Here, stead-state flow condition with constant water content and water flux was assumed, the analytic solution for Eq. (1) is as follows (Wang et al., 2000):

$$C(t) = \frac{M}{Qt_0}\frac{1}{\sqrt{4\pi P\left(\frac{t}{t_0}\right)^3}} exp\left[-\frac{\left(1-\frac{t}{t_0}\right)^2}{4P\frac{t}{t_0}}\right] \tag{3}$$

where t_0 is the mean transit time ($t_0 = x/v$), P is the dispersion parameter ($P = D_L t_0/x^2$). M is the mass of injected tracer amount [M], Q is the flow rate [$L^{-3}\,T^{-1}$] The dispersivity is inversely estimated using the measured tracer breakthrough curves from the column experiments, by minimizing the root mean square error (RMSE).

$$\mathrm{RMSE} = \sqrt{\frac{\sum_{i=1}^{n}(P_i - O_i)^2}{n}} \tag{4}$$

where P_i is the predicted tracer concentration [ML^{-3}], O_i is the observed tracer concentration [ML^{-3}], and n is the number of observations [−]. The transport parameter values information for simulating tracer experiments was provided in the SI Table S1.

2.4.2. Microplastic transport

Previous studies have shown that MPs are mostly retained on the surface layer and the deposited amount decreases gradually (Bradford et al., 2005; Dong et al., 2018). This transport mechanism is described by coupling the advection-dispersion equation with two-site sorption kinetics with first-order attachment-detachment coefficients and depth-dependent blocking function:

$$\theta\frac{\partial C}{\partial t} + p_b\frac{\partial S_1}{\partial t} + p_b\frac{\partial S_2}{\partial t} = \theta\left(D_L\frac{\partial^2 C}{\partial x^2} - v\frac{\partial C}{\partial x}\right) \tag{5}$$

$$p_b\frac{\partial S_1}{\partial t} = \theta K_{att1} C \tag{6}$$

$$p_b\frac{\partial S_2}{\partial t} = \theta K_{att2}\Psi C - p_b K_{det2} S_2 \tag{7}$$

$$\Psi = \left(\frac{d_{50}+x}{d_{50}}\right)^{-\beta} \tag{8}$$

where θ is the volumetric water content [L^3L^{-3}], p_b is the soil bulk density [M L^{-3}], S is the MPs concentration in solid phase [M M^{-1}] (1 and 2 indicate the kinetic sorption site), v is the pore water velocity [L T^{-1}]. K_{att} is the first-order attachment coefficient [T^{-1}], K_{det} is the first-order detachment coefficient [T^{-1}], d_{50} is the median diameter of sediments [L], β is the empirical factor that controls the shape of the MPs Retention Profiles (RPs) [−], which is set as 0.432 (Bradford et al., 2003). Ψ modulates the MP blocking in the porous medium [−]. The deposition in the first kinetic site is assumed to be irreversible with $K_{det} = 0$. For the second site, reversible deposition is considered with a depth-dependent blocking function applied to control the transport behavior of MPs (Li et al., 2024).

The finite element model HYDRUS-1D was used to solve Eq. (5), and combined with the observed breakthrough curves and RPs to inversely estimate the MPs transport parameters using the Levenberg-Marquardt nonlinear least squares optimization algorithm. In particular, the dispersivity of the MPs, the attachment coefficient for both sites and the detachment coefficient for the second site were optimized. The optimization algorithm minimizes the sum of squared residuals between observations and model predictions. Finally, the model fitting accuracy was evaluated using the determination coefficient (R^2).

2.5. Quality assurance and control

Glass vials and beakers were well-cleaned and checked under a UV lamp to ensure no cross-contamination. Cotton lab coats and leather gloves were worn during the entire lab experiments, sample preparation, and analysis. A stainless-steel spoon was used to collect soil samples and glass stickers were applied to stir the samples with filtrated NaCl solution (no applied MP found) during density separation. Density separation was operated in a fume hood with aluminum foils employed to cover the samples until processed to the filtration process.

An extraction recovery test was conducted to examine the applied MP analytic methods; details can be found in SI Table S2. Briefly, a known amount of MPs was introduced into beakers packed with gravel or glass beads, and then followed the extraction and filtration process as described above. The number of MPs was counted with confocal microscopy and the software ImageJ. The extraction efficiency was obtained based on the number of extracted MPs compared to the spiked MPs number. The recovery rate was 85.47 ± 5.31%, 101.83 ± 6.55%, and 95.59 ± 2.36% for MPs of density of 0.995 cm^{-3}; 1.0 g cm^{-3}; and 1.12 g cm^{-3}, respectively from gravel. In beaks spiked with glass beads, the recovery rate was 93.40 ± 1.19% (0.995 cm^{-3}), 95.03 ± 4.61% (1 g cm^{-3}), and 100.21 ± 4.52% (1.12 cm^{-3}).

3. Results

3.1. Transport of deuterium tracer

The observed and simulated tracer breakthrough curves in columns packed with gravel and glass beads are shown in Fig. 1 (A, B). The concentration data were normalized to the input tracer mass to facilitate the comparison between column experiments. The recovery of tracer is 97.95 ± 2.25% and 97.91 ± 3.09% in columns with gravel and glass beads, respectively (Fig. 1B). The simulated tracer concentrations agree with observations with a minimum RMSE value of 0.018 and 0.0013 L^{-1} for tracers in columns packed with gravel and glass beads, respectively, thus suggesting a good fitting accuracy of the model. The mean transit time for the tracer in the glass beads column (35 min) is slightly earlier than it is in columns packed with gravel (40 min), and the observed maximum normalized concentration of deuterium is higher in column with glass beads (21.06 ± 3.14 L^{-1}) compared to gravel columns (16.87 ± 2.25 L^{-1}). This agrees with the tracer-derived dispersivity, which was found to be smaller in the uniform glass bead columns (α_L = 0.275 cm) compared to the gravel (α_L = 0.45 cm) showing a wider distribution of pore water velocities.

3.2. Density-dependent MP transport in porous media

3.2.1. Mass balance

The MP mass recovery rate was obtained by combining MP concentration in effluent and porous media (Fig. 2A). As shown in Table 1,

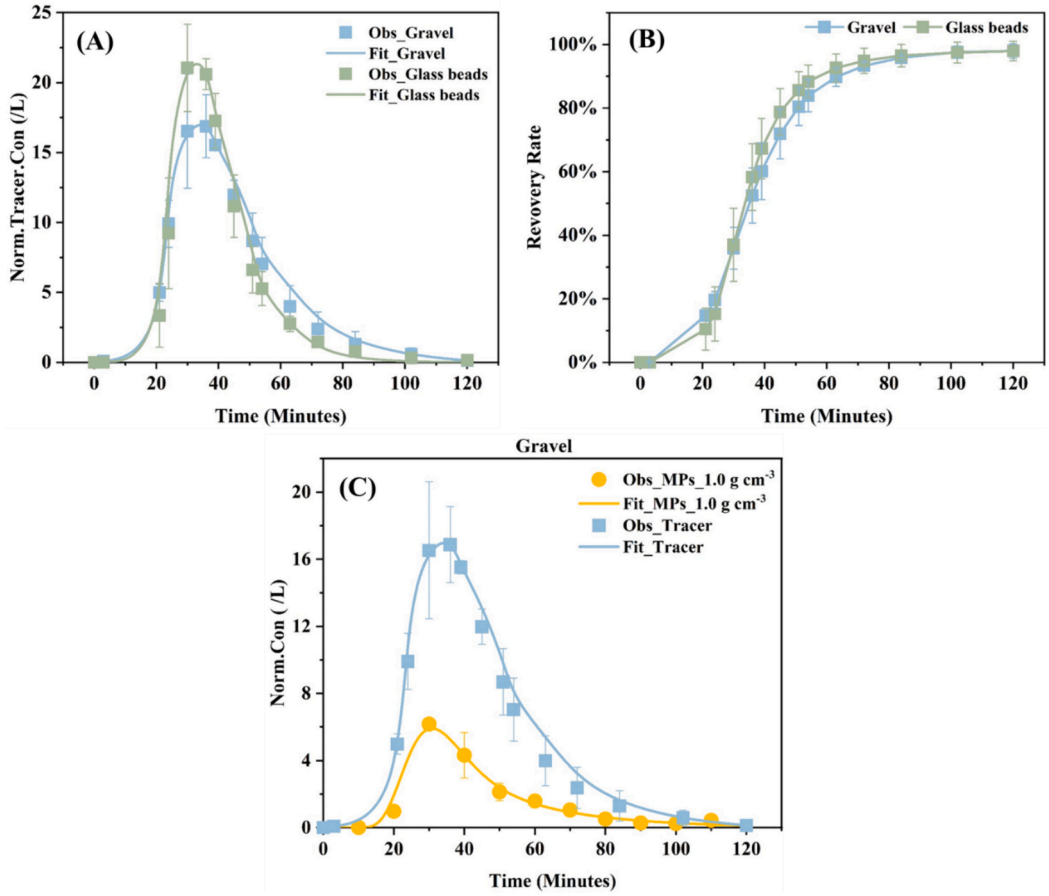

Fig. 1. Observed (symbols) and fitted (lines) conservative tracer (deuterium) breakthrough curves (A) and recovery rates (B) in columns packed with gravel and glass beads. Observed and fitted breakthrough curves of tracer and MPs (27–32 μm, 1.0 g cm^{-3}) in columns packed with gravel (C). The sampling interval was 3 min for tracer and 10 min for microplastics. The error bars represent the standard deviation between duplicate column experiments.

more neutrally buoyant MPs (1 g cm^{-3}, 22.9 ± 4.3%) are present in the effluent compared to buoyant (0.995 g cm^{-3}, 6.0 ± 1.1%) and sinking MPs (1.12 g cm^{-3}, 0.1 ± 0.0%). Furthermore, results show that sinking MPs are mainly retained in the packed columns (95.5 ± 1.4% in gravel). A similar behavior was also observed in columns packed with glass beads (Fig. 2B). Finally, it is worth mentioning that significant amounts of all types of MPs (> 70%, Table 1) were retained in the columns even though both MPs and porous media are negatively charged (unfavorable attachment condition with electrostatic repulsion energy).

3.2.2. MPs breakthrough curves

The observed breakthrough curves of MPs of different densities in the effluent indicate that MP transport is sensitive to changes in particle density (Fig. 2 C and D). In columns packed with gravel, the peak concentration decreased from 12 ± 0.54 μg mL^{-1} for neutral to 3.2 ± 0.11 μg mL^{-1} for buoyant, to 0.044 ± 0.002 μg mL^{-1} for sinking MPs. As expected from mass balance information, similar breakthrough curves of MPs with certain densities were observed as presented in Fig. 2D.

3.2.3. Retention profile

The observed RPs of MPs of different densities were plotted in Fig. 2 (E, F) for gravel and glass beads columns, respectively. Consistent with mass balance information, more sinking MPs were deposited within the packed columns, followed by buoyant and neutral MPs. Additionally, greater mass retention of sinking MPs was observed near the column inlet compared to neutrally and buoyant MPs, then decreasing with depth to a more constant concentration. For all MPs, the majority of the input MPs remained in the first 2 cm of packed columns. The amounts of deposited MPs then decreased gradually or more or less constant with increasing travel distance. The MP (1 g cm^{-3}) concentration in columns packed with porous media changed from 3.43E-06 ± 2.04E-07 at 3 cm, to 3.29E-06 ± 1.16E-07 at 4 cm and 2.90E-06 ± 1.42E-08 at 5 cm. Similar trends were observed for MPs of different densities in different porous media. The detected concentration of MPs of different densities within columns packed with different porous media can be found in SI Table S3.

3.3. Modeling results

The two-site kinetic transport model with a depth-dependent blocking function (Bradford et al., 2002; Li et al., 2024) was employed to simulate the breakthrough curves and retention profiles (Fig. 2C-F). The value of simulated dispersivity for MPs in different porous media is listed in Table 2. The resulting dispersivity is similar for MPs of specific density in columns packed with gravel and glass beads, except for sinking MPs. The fitted K_{att} and K_{det} were different for the tested MPs (Fig. 3, Table 2). The K_{att} is associated with the experimental results, neutral MPs with the lowest K_{att1} (0.05 ± 0.0017 min^{-1}) value indicate that neutral MPs are most mobile in comparison with 0.095 ± 0.0019 min^{-1} for buoyant MPs and 0.25 ± 0.0057 min^{-1} for sinking MPs. K_{att2} for MPs of different densities follow the same order (sinking > buoyant > neutral MPs) in columns packed with gravel and glass beads. Additionally, both attachment coefficients (K_{att1} and K_{att2}) had the same order of magnitude (Table 2) with K_{att1} (irreversible attachment) being slightly greater than the reversible attachment (K_{att2}) except for the sinking MPs. Furthermore, the fitted K_{att1} values were similar in gravel and glass bead columns for MPs with a specific density. Interestingly, the detachment coefficient K_{det} for the sinking MPs was high, though wide

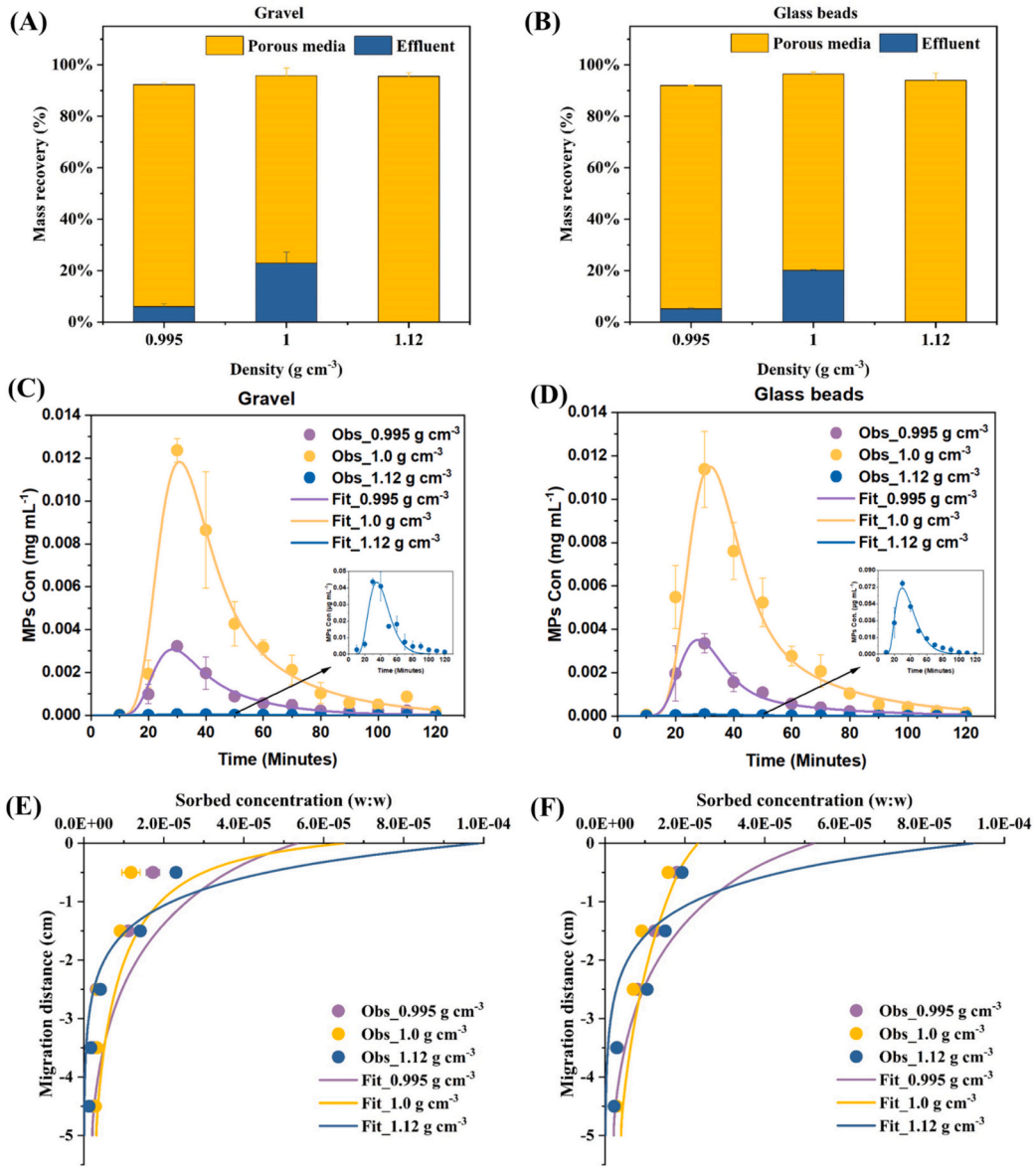

Fig. 2. Recovered microplastic mass in effluent and solid phase in saturated columns packed with gravel (a) and glass beads (b). Observed (noted as Obs, symbols) and fitted (noted as Fit, curves) MP breakthrough curves (c, d) and retention profiles (e, f) of MPs in different densities. Note the unit of MP (1.12 g cm^{-3}, in blue) concentration changed from mg mL^{-1} to μg mL^{-1} within the subgraph of (C) and (D).

confidence intervals suggest high uncertainty in the estimation of this parameter (Fig. 3B, Table 2).

4. Discussion

4.1. Transport of tracer and MPs

The peak of neutral MPs (1.0 g cm^{-3}) arrived earlier compared to the conservative tracer mainly for the experiments using gravel (Fig. 1C), which is consistent with previous studies due to size exclusion (Bradford et al., 2002; Li et al., 2024). As suggested by earlier findings (Bradford et al., 2002; Keller et al., 2004), the tracer and colloids might follow different flow paths. Therefore, we followed the recommendations by Chrysikopoulos and Katzourakis (2015) and fitted MP-specific dispersity. Indeed, the resulting dispersivity is different for MPs (0.06–0.20 cm) and tracer (0.45 cm) in the gravel sediment. This can be explained by the fact that the tracer flows through the entire pore system (including also diffusion), thus exhibiting a larger dispersivity compared to MPs, which follow only those flow paths through larger pores and are excluded from smaller pores due to MPs' size (Niehren and Kinzelbach, 1998; Sirivithayapakorn and Keller, 2003). This effect is less pronounced in the glass beads with more uniform pore size distributions resulting in slightly different dispersivities for MPs (0.17–0.33 cm) and tracer (0.275 cm). Conversely, larger dispersivity of suspended silt particles (2–30 μm) was observed compared to conservative tracer (fluorescein) by Ahfir et al. (2007). This inconsistent finding might be attributed to the larger size distribution of the suspended silt particles.

Compared to the high recovery of the tracer (97.95 ± 2.25%), fewer MPs (22.89 ± 4.34%) were recovered, which can be explained by different retention mechanisms within the porous sediments. This again suggests that the tracer and MPs were not transported in the same flow path, supporting the choice of fitting a MP specific dispersivity from the observed experimental results.

Table 2
Summary of results from HYDRUS-1D simulations using a two-site kinetic transport model with a depth-dependent blocking model (first site: attachment, second site: attachment-detachment with depth-dependent blocking function; K_{att_1} and K_{att_2} represent the attachment coefficient in the first and second kinetic sites. K_{det_2} is the detachment coefficient in the second sites; S.E.Coeff is the standard error coefficient for the estimated parameters).

Density	Dispersivity	S.E. Coeff	First site				Second site								R^2
			K_{att_1}	S.E. Coeff	95 % Confidence limits		K_{att_2}	S.E. Coeff	95 % Confidence limits		K_{det_2}	S.E. Coeff	95 % Confidence limits		
g cm^{-3}	min		min^{-1}		Lower	Upper	min^{-1}		Lower	Upper	min^{-1}		Lower	Upper	
0.995	2.01E-01	4.15E-03	9.55E-02	1.85E-03	9.15E-02	9.95E-02	5.89E-02	8.69E-03	4.02E-02	7.75E-02	8.39E-02	2.08E-02	4.02E-02	7.75E-02	0.99707
1	1.99E-01	9.80E-03	5.07E-02	1.73E-03	4.70E-02	5.44E-02	3.96E-02	5.82E-03	2.71E-02	5.21E-02	5.50E-02	1.60E-02	2.08E-02	8.92E-02	0.99218
1.12	5.90E-02	1.18E-02	2.47E-01	5.72E-03	2.34E-01	2.59E-01	5.43E-01	2.11E-01	8.96E-02	9.97E-01	3.33E-01	1.40E-01	3.32E-02	6.33E-01	0.87448

Glass beads															
Density	Dispersivity	S.E. Coeff	First site				Second site								R^2
			K_{att_1}	S.E. Coeff	95 % Confidence limits		K_{att_2}	S.E. Coeff	95 % Confidence limits		K_{det_2}	S.E. Coeff	95 % Confidence limits		
g cm^{-3}	min		min^{-1}		Lower	Upper	min^{-1}		Lower	Upper	min^{-1}		Lower	Upper	
0.995	2.77E-01	6.96E-03	9.36E-02	1.60E-03	9.01E-02	9.70E-02	3.70E-02	4.16E-03	2.81E-02	4.60E-02	4.44E-02	1.05E-02	2.20E-02	6.69E-02	0.98691
1	3.29E-01	9.36E-03	4.66E-02	2.81E-03	4.06E-02	5.26E-02	3.40E-02	7.96E-03	1.70E-02	5.11E-02	4.61E-02	2.31E-02	-3.35E-03	9.56E-02	0.99458
1.12	1.72E-01	1.53E-02	2.23E-01	3.84E-03	2.15E-01	2.31E-01	2.21E-01	4.84E-02	1.18E-01	3.25E-01	1.96E-01	5.12E-02	8.61E-02	3.06E-01	0.91293

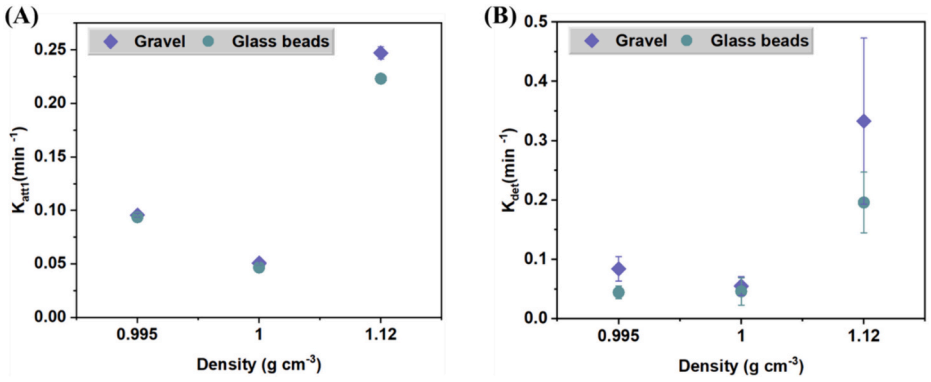

Fig. 3. Fitted K_{att1} (A) and K_{det} (B) with two-site sorption kinetics with first-order attachment-detachment coefficients and depth-dependent blocking function for MPs of different densities flowing through columns packed with gravel and glass beads. K_{att1} represents the attachment coefficient in the first kinetic site, and K_{det} represents the detachment coefficient. Note different Y-axis scales in Panel (A) and Panel (B).

4.2. Transport of MPs in natural sediments and uniform glass beads

The high mass recoveries of MPs (Fig. 2A, B) indicate that applied measurement and analytic methods were reliable. The small difference between results from duplicated columns can be a reason for the packing difference. A similar amount of retained MP mass in columns packed with gravel and glass beads suggests that surface properties (e.g., roughness) do not significantly influence the transport of MPs in this work. This agrees with results from an earlier studies showing that surface roughness heterogeneity cannot explicitly account for MP retention in the presence of energy barrier (Pazmino et al., 2014). This is further supported by previous findings that reported similar breakthrough curves of PS microspheres in quartz sand and glass beads at 0.01 and 0.001 M (molarity, moles L^{-1}) (Shen et al., 2011). Surface roughness plays a significant role only at high ionic strength conditions (Shen et al., 2011), which is not the case for this work, as the experiment was conducted at low ionic strength applying tap water. The equivalent breakthrough curves of MPs of certain densities (Fig. 2C, D) further support that the surface roughness of porous media did not obviously influence the transport of MPs under tested conditions. However, these findings are different from those from Tong and Johnson (2006), who observed higher collision efficiency of PS MPs in quartz sand compared to that in glass beads under favorable attachment conditions (both MPs and porous media were oppositely charged). These different findings further suggest that other, unknown factors might impact the fate and deposition of MP in different porous media.

The recovered mass of sinking MPs at the first 1 cm in gravel is slightly more than it is in glass beads, and the form of the retention profiles was more clearly of hyper-exponential shape. This result can be explained by a rougher surface of natural sediments, which reduce the mobility of MPs with potentially increased interactions between MPs and porous media (Shen et al., 2011). However, a comparable total mass of remaining MPs was observed in columns packed with glass beads and gravel, indicating that surface roughness does not play a main role in determining MP mobility in this work.

4.3. Transport of MPs of different densities

Particle density affected the transport behavior of MPs in saturated porous media. In particular, the mobility of MPs followed the order of particle density 1.0 g cm^{-3} > 0.995 g cm^{-3} > 1.12 g cm^{-3} in all columns (Fig. 2B, C). Therefore, the assumption that higher mobility of high-density MPs in porous media systems due to higher settling rates in aquatic environment does actually not hold true. Buoyant forces influenced the transport of buoyant MPs (0.995 g cm^{-3}) by acting against the downward movement of MPs in saturated media. This is further supported by the lower amount of buoyant MPs leached from the columns than neutral MPs (1.0 g cm^{-3}). Conversely, sinking MPs (1.12 g cm^{-3}) have higher settling velocities based on Stokes' law, thus enhancing retention with increased contact possibility (gravitational sedimentation) within the porous media in the columns. This agrees with a previous modeling study, in which Polyethylene terephthalate (PET) MPs with high density were more likely to deposit in riverine systems (Lu et al., 2023). Field observations conducted by Soltani et al. (2022) also found that PET MPs were the dominant polymer type retained in sediment samples. However, this differs from what Lin et al. (2018) observed, that light PE and polypropylene (PP) MPs were the dominant polymer types found in the water and sediment samples. This might be explained by the selected density separation solution with density around 1.2 g cm^{-3}, which then eliminated the detection possibility of dense MPs (PET, Polyvinyl chloride PVC and etc.).

In addition to particle density, flow velocity has been discussed as an influencing factor in MP transport patterns (Fei et al., 2022; Torkzaban et al., 2008). In column experiments, an increased mass of PS MPs was recovered in the effluent when water velocity increased from 0.35 to 0.87 cm min^{-1} (Torkzaban et al., 2008). Additionally, decreased deposition efficiencies of PS MPs with increasing flow velocity under conditions that electrostatic repulsion exists, have been reported in several publications (Johnson et al., 2007; Keller et al., 2004; Tong and Johnson, 2006), implying that water flow influences MP mobility which was, however not tested in our study as we wanted to focus on density only. Still, more experiments would be required to systematically test the density-impacted transport of MPs for different flow rates and in different sediment types.

Besides, gravity has been discussed to influence the transport of engineered nanoparticles (metal-oxide NPs), because slightly lower peak concentrations were observed under down-flow compared to up-flow orientation (Cai et al., 2015). However, a negligible effect of gravity on carbon-based NPs (lighter in density, and smaller in size) was noticed in both flow directions (Cai et al., 2015). This indicates that gravity has a more pronounced impact on the transport of denser, larger particles (Ma et al., 2011). In our study, gravity acted in the same direction of flow, and therefore, it can be concluded that the decreased mobility of sinking MPs (1.12 g cm^{-3}, 27–32 μm) is mainly caused by the gravitational sedimentation, which favors the entrapment of particles in soil pores due to the interaction between MPs and the surface of porous media, thus reducing the amounts of MPs transported with the water flow. Moreover, longer residence time under a lower flow rate can also reduce the transport of sinking MPs, which was observed by 3–4% higher deposition rate of PS MPs with flow rate changes from 3 to 0.06 ml min^{-1} (Chen et al., 2010). Conversely, buoyant forces act as lift force against gravitational sedimentation, drive MPs away from collector surface to bulk fluids, and thus reduce the entrapment of MPs in soil pores. This can be the reason why we found that more buoyant MPs were transported through packed columns compared to sinking MPs in our study.

4.4. Retention of MPs of different densities

Fine particles (< 10 μm) are controlled by Brownian diffusion, van der Waals forces, and electrostatic effects (Bennacer et al., 2017; Frey et al., 1999), whereas sedimentation and interception contribute to the retention of larger particles (Bradford et al., 2003). This is consistent with other observations from a flow chamber system where the deposition of PS MPs (> 1 μm) was mainly driven by gravity (Chen and Bai, 2012) and from experiments on the deposition of PS MPs and bacteria larger than 1 μm which were dominated by gravity, and not diffusion-based (Chen et al., 2010). Furthermore, it was shown that sedimentation dominated the deposition of silt particles (2.65 g cm^{-3}) under low flow rates, and the increased hydrodynamic forces with increasing flow rate inhibited the deposition of particles by overcoming gravity forces (Ahfir et al., 2007). This indicates that gravity is a considerable mechanism for MP deposition, which should also be the case for our study; especially under low flow rates (0.05 cm min^{-1}) that are typical for groundwater and used in our study. Still, we only tested one constant flow rate in this work, and coupled effects of multiple processes in dependence on flow rates would need to be tested in the future studies, to identify the mechanisms of density-related retention for sinking or buoyant MPs in porous media.

The general form of the retention profiles is consistent with previous observations finding that a significant mass of MPs was retained in the upper sediment layer decreasing with depth (Bradford et al., 2002). Also, the deposition rate of micro-sized glass particles (2.4 g cm^{-3}) decayed with flow distance, then became constant (Yiantsios and Karabelas, 1998). The determination of straining in influencing MP mobility can be supported by looking at the ratio between particle diameter and diameter of porous media (d_p/d_{50}) (Bradford et al., 2006). This ratio is 0.96% in our study, which is larger than the threshold value (0.2%) defined by Bradford et al. (2003) and 0.5% suggested by (Bradford et al., 2004). This suggests that straining is one of the main mechanisms for MP retention due to size exclusion, which prohibits the movement of MPs by pore sizes, thus MPs can only bypass through larger pores (Bradford et al., 2003). Besides straining, attachment can also be an important mechanism for the deposition of MPs; mainly in deeper layers, as a more uniform change of retained MPs mass with depth >2 cm was observed in our study. This is supported by previous findings of a similar magnitude of retained MP mass in the region with constant retention (Bradford et al., 2002).

4.5. Model limitation

Results from HYDRUS-1D indicate that the model can describe MP effluent concentration for different densities and porous media (Fig. 2C-F), with the tails of MP breakthrough curves well predicted. The goodness of model fit can be further supported by the high R^2 values. The K_{att} value increase with particle density, indicating that the particle density influenced the transport behavior of MPs under saturated conditions. K_{det} were higher for sinking MPs compared to others which was necessary to explain the observed tailing effect of experimental data, indicating a higher likelihood of detachment of sinking MPs from the collector surface to bulk fluids. Also, the higher value of standard error (S.E) of K_{det} of sinking MPs suggests that the output of the model is insensitive to changes in K_{det}. Note that the same order of magnitude of K_{att} and K_{det} was observed, which is in line with another study focusing on PS MP mobility in different sands (Leij and Bradford, 2013). These results suggested that the attachment of MPs on both sites approached equilibrium as suggested by Xing et al. (2020). This differs from another finding, that K_{att} is several orders of magnitude higher than K_{det} (Bradford and Bettahar, 2006).

The two-site kinetic transport model with a depth-dependent blocking function provides a reasonable description of the concentration in the effluent. However, the retention profiles from the experimental data did not fit with model predictions, especially for the mass of MPs in the upper layers. The applied model overestimated the retained mass of MPs near the column inlet. One reason might be the fact that MP mixtures were introduced into the same column simultaneously, and therefore, competition on deposition sites cannot be excluded. Further, other factors like density-driven transport are not included in the model

description, and we are not aware of any other model that does so. Nevertheless, the two-site kinetic transport model with a depth-dependent blocking function describes the effluent concentration of MPs fairly well but does not satisfactorily describe MPs retention for different densities in porous media. This indicates that more rigorous modeling approaches are required to explore the role of particle density on MP mobility.

4.6. Environmental implication

We have examined the fate of MPs of different densities in different porous media and quantified processes with a transport model. The experimental data demonstrate that particle density does affect the transport behavior of MPs. And the higher sinking rate of denser MPs in aquatic systems does not hold true for higher mobility in porous media systems. Neutral MPs were more mobile compared to buoyant MPs, which again were more mobile compared to sinking MPs. This further suggests that (i) differently dense particles can behave differently in porous media and (ii) MPs can change their transport behavior in porous media if the density is altered during their lifetime. The latter has already been shown in previous studies. For example, long-term colonization by microorganisms can alter the apparent density of plastic particles (Lobelle and Cunliffe, 2011), thus changing the distribution pattern of MPs in environmental compartments and resulting in the predominantly finding buoyant PE and PP polymer types in surface water systems (Schwarz et al., 2019). Also, biofouling has been discussed to influence plastic properties (surface charge, hydrophobicity, density), thus altering their fate in the environment (Kooi et al., 2017; Ye and Andrady, 1991). Previous study found that the sinking rate of MPs incorporated with phytoplankton aggregates was significantly increased compared to free PS beads (Long et al., 2015). Another potential density-altering mechanism is the sorption of persistent organic pollutants (e.g., pesticides, antibiotics) on MPs (Li et al., 2021; Rong et al., 2023; Wang et al., 2022), which can facilitate their mobility in the environment (Grego et al., 2022; Mistri et al., 2017; Wang et al., 2017; Yang et al., 2021).

The density-dependent effect on the mobility of MPs could also be an option to actually mitigate their transport distances in porous media. Based on the observed high retention of sinking MPs in our work, the mobility of MPs could be reduced by increasing MPs' density. This would be possible by identifying suitable agents that can be applied at contaminated sites. The remediation technique would rely on using agents that increase the density of MPs or decrease the density of the fluid, resulting in the demobilization of MP and preventing further MP downstream pollution in subsurface systems. Additionally, findings from our work could provide insights into removing MPs from sewage during wastewater treatment processes. Adequate coagulants or flocculants can be utilized during the primary and secondary treatment to alter the density of MPs, hence promoting the settling of MPs. This could reduce the risk of reintroducing MPs to other environmental compartments through direct discharge or application of treated wastewater.

5. Summary and conclusion

Experimental and simulated results were presented to describe the effect of particle density on the transport of MPs under saturated conditions. Results show that density does influence the transport of MPs in two tested sediment types. Sinking MPs are mainly retained in the sediment, and neutral MPs were more mobile compared to sinking and buoyant MPs under the tested flow rate, which is representative of porous groundwater media. If these density-dependent findings change with flow rate remain to be tested. The two-site kinetic transport model with a depth-dependent blocking function described the observed MP transport; particularly the effluent concentrations. However, this model does not account for processes related to the particle density, and therefore, discrepancies between observed and fitted RPs with the applied model were noticed. This emphasizes the importance of analyzing not only MP concentrations in the effluent but also in the sediment. Those data are required to systematically identify mechanisms influencing the density-impacted retention of MPs in porous media and to develop adequate models describing those processes and thus the fate of MPs in porous media; not only for spheres but for any type of MPs and by considering processes that alter the MPs' density during their lifetime in the environment.

CRediT authorship contribution statement

Wang Li: Writing – review & editing, Writing – original draft, Visualization, Validation, Software, Methodology, Formal analysis, Data curation, Conceptualization. **Giuseppe Brunetti:** Writing – review & editing, Methodology, Formal analysis, Conceptualization. **Anastasiia Bolshakova:** Writing – review & editing, Methodology. **Christine Stumpp:** Writing – review & editing, Supervision, Resources, Project administration, Methodology, Funding acquisition, Conceptualization.

Declaration of competing interest

The authors declare that they have no known competing financial interests or personal relationships that could have appeared to influence the work reported in this paper.

Data availability

Data will be made available on request.

Acknowledgments

We would like to thank Ms. Martina Faulhammer and Ms. Stefanie Grabner for their help in the lab for isotope measurement, The confocal laser scanning microscopy (SP8, Leica) was kindly provided by the BOKU Core Facility Multiscale Imaging. This study was supported by the project SOPLAS, which has received funding from the European Union's Horizon 2020 research and innovation programme under the Marie Skłodowska-Curie grant agreement No 955334. The authors acknowledge that open access funding is provided by University of Natural Resources and Life Sciences Vienna (BOKU).

Appendix A. Supplementary data

Supplementary data to this article can be found online at https://doi.org/10.1016/j.scitotenv.2024.173429.

References

Ahfir, N.-D., Wang, H.Q., Benamar, A., Alem, A., Massei, N., Dupont, J.-P., 2007. Transport and deposition of suspended particles in saturated porous media: hydrodynamic effect. Hydrogeol. J. 15 (4), 659–668. https://doi.org/10.1007/s10040-006-0131-3.

Ahmadi, P., Elagami, H., Dichgans, F., Schmidt, C., Gilfedder, B.S., Frei, S., Peiffer, S., Fleckenstein, J.H., 2022. Systematic evaluation of physical parameters affecting the terminal settling velocity of microplastic particles in lakes using CFD. Front. Environ. Sci. 10. https://www.frontiersin.org/articles/10.3389/fenvs.2022.875220.

Becker, M.W., Coplen, T.B., 2001. Use of deuterated water as a conservative artificial groundwater tracer. Hydrogeol. J. 9 (5), 512–516. https://doi.org/10.1007/s100400100157.

Bennacer, L., Ahfir, N.-D., Alem, A., Wang, H., 2017. Coupled effects of ionic strength, particle size, and flow velocity on transport and deposition of suspended particles in saturated porous media. Transp. Porous Media 118 (2), 251–269. https://doi.org/10.1007/s11242-017-0856-6.

Bläsing, M., Amelung, W., 2018. Plastics in soil: analytical methods and possible sources. Sci. Total Environ. 612, 422–435. https://doi.org/10.1016/j.scitotenv.2017.08.086.

Bradford, S.A., Bettahar, M., 2006. Concentration dependent transport of colloids in saturated porous media. J. Contam. Hydrol. 82 (1), 99–117. https://doi.org/10.1016/j.jconhyd.2005.09.006.

Bradford, S.A., Yates, S.R., Bettahar, M., Simunek, J., 2002. Physical factors affecting the transport and fate of colloids in saturated porous media. Water Resour. Res. 38 (12) https://doi.org/10.1029/2002WR001340, 63–1.

Bradford, S.A., Simunek, J., Bettahar, M., van Genuchten, M.Th., Yates, S.R., 2003. Modeling colloid attachment, straining, and exclusion in saturated porous media. Environ. Sci. Technol. 37 (10), 2242–2250. https://doi.org/10.1021/es025899u.
Bradford, S.A., Bettahar, M., Simunek, J., van Genuchten, M.Th., 2004. Straining and attachment of colloids in physically heterogeneous porous media. Vadose Zone J. 3 (2), 384–394. https://doi.org/10.2136/vzj2004.0384.
Bradford, S.A., Simunek, J., Bettahar, M., Tadassa, Y.F., van Genuchten, M.T., Yates, S.R., 2005. Straining of colloids at textural interfaces. Water Resour. Res. 41 (10) https://doi.org/10.1029/2004WR003675.
Bradford, S.A., Simunek, J., Bettahar, M., van Genuchten, M.T., Yates, S.R., 2006. Significance of straining in colloid deposition: evidence and implications. Water Resour. Res. 42 (12) https://doi.org/10.1029/2005WR004791.
Büks, F., Kaupenjohann, M., 2020. Global concentrations of microplastics in soils – a review. SOIL 6 (2), 649–662. https://doi.org/10.5194/soil-6-649-2020.
Cai, L., Zhu, J., Hou, Y., Tong, M., Kim, H., 2015. Influence of gravity on transport and retention of representative engineered nanoparticles in quartz sand. Fate and Transport of Biocolloids and Nanoparticles in Soil and Groundwater Systems 181, 153–160. https://doi.org/10.1016/j.jconhyd.2015.02.005.
Chen, G., Hong, Y., Walker, S.L., 2010. Colloidal and bacterial deposition: role of gravity. Langmuir : The ACS J. Surf. Colloids 26 (1), 314–319. https://doi.org/10.1021/la903089x.
Chen, X., Bai, B., 2012. Effect of gravity on transport of particles in saturated porous media. Chin. J. Geotech. Eng. 34 (9), 1661–1667.
Chrysikopoulos, C.V., Katzourakis, V.E., 2015. Colloid particle size-dependent dispersivity. Water Resour. Res. 51 (6), 4668–4683. https://doi.org/10.1002/2014WR016094.
Dong, Z., Qiu, Y., Zhang, W., Yang, Z., Wei, L., 2018. Size-dependent transport and retention of micron-sized plastic spheres in natural sand saturated with seawater. Water Res. 143, 518–526. https://doi.org/10.1016/j.watres.2018.07.007.
Fei, J., Xie, H., Zhao, Y., Zhou, X., Sun, H., Wang, N., Wang, J., Yin, X., 2022. Transport of degradable/nondegradable and aged microplastics in porous media: effects of physicochemical factors. Sci. Total Environ. 851, 158099 https://doi.org/10.1016/j.scitotenv.2022.158099.
Fei, J., Cui, J., Wang, B., Xie, H., Wang, C., Zhao, Y., Sun, H., Yin, X., 2023. Co-transport of degradable microplastics with cd(II) in saturated porous media: synergistic effects of strong adsorption affinity and high mobility. Environ. Pollut. 330, 121804 https://doi.org/10.1016/j.envpol.2023.121804.
Frey, J.M., Schmitz, P., Dufreche, J., Gohr Pinheiro, I., 1999. Particle deposition in porous media: analysis of hydrodynamic and weak inertial effects. Transp. Porous Media 37 (1), 25–54. https://doi.org/10.1023/A:1006546717409.
Fuller, S., Gautam, A., 2016. A procedure for measuring microplastics using pressurized fluid extraction. Environ. Sci. Technol. 50 (11), 5774–5780. https://doi.org/10.1021/acs.est.6b00816.
Gerba, C.P., Keswick, B.H., 1981. Survival and transport of enteric viruses and Bacteria in groundwater. In: van Duijvenbooden, W., Glasbergen, P., van Lelyveld, H. (Eds.), Studies in Environmental Science, vol. 17. Elsevier, pp. 511–515. https://doi.org/10.1016/S0166-1116(08)71944-7.
Gramling, C.M., Harvey, C.F., Meigs, L.C., 2002. Reactive transport in porous media: a comparison of model prediction with laboratory visualization. Environ. Sci. Technol. 36 (11), 2508–2514. https://doi.org/10.1021/es0157144.
Grego, M., Viršek, M.K., Bajt, O., 2022. 2—Microplastics in seawater and sediments—Distribution and transport. In: Bonanno, G., Orlando-Bonaca, M. (Eds.), Plastic Pollution and Marine Conservation. Academic Press, pp. 31–73. https://doi.org/10.1016/B978-0-12-822471-7.00002-X.
Han, N., Zhao, Q., Ao, H., Hu, H., Wu, C., 2022. Horizontal transport of macro- and microplastics on soil surface by rainfall induced surface runoff as affected by vegetations. Sci. Total Environ. 831, 154989 https://doi.org/10.1016/j.scitotenv.2022.154989.
Harvey, R.W., Garabedian, S.P., 1991. Use of colloid filtration theory in modeling movement of bacteria through a contaminated sandy aquifer. Environ. Sci. Technol. 25 (1), 178–185. https://doi.org/10.1021/es00013a021.
Hu, C., Lu, B., Guo, W., Tang, X., Wang, X., Xue, Y., Wang, L., He, X., 2021. Distribution of microplastics in mulched soil in Xinjiang, China. Int. J. Agric. Biol. Eng. 14 (2), 196–204. Natural Science Collection; Publicly Available Content Database. 10.25165/j.ijabe.20211402.6165.
Jarvie, H.P., Al-Obaidi, H., King, S.M., Bowes, M.J., Lawrence, M.J., Drake, A.F., Green, M.A., Dobson, P.J., 2009. Fate of silica nanoparticles in simulated primary wastewater treatment. Environ. Sci. Technol. 43 (22), 8622–8628. https://doi.org/10.1021/es901399q.
Jiang, Y., Yin, X., Xi, X., Guan, D., Sun, H., Wang, N., 2021. Effect of surfactants on the transport of polyethylene and polypropylene microplastics in porous media. Water Res. 196, 117016 https://doi.org/10.1016/j.watres.2021.117016.
Johnson, P.R., Elimelech, M., 1995. Dynamics of colloid deposition in porous media: blocking based on random sequential adsorption. Langmuir 11, 801–812.
Johnson, W.P., Li, X., Assemi, S., 2007. Deposition and re-entrainment dynamics of microbes and non-biological colloids during non-perturbed transport in porous media in the presence of an energy barrier to deposition. Biological Processes in Porous Media: From the Pore Scale to the Field 30 (6), 1432–1454. https://doi.org/10.1016/j.advwatres.2006.05.020.
Johnson, W.P., Rasmuson, A., Pazmiño, E., Hilpert, M., 2018. Why variant colloid transport behaviors emerge among identical individuals in porous media when colloid–surface repulsion exists. Environ. Sci. Technol. 52 (13), 7230–7239. https://doi.org/10.1021/acs.est.8b00811.
Keller, A.A., Sirivithayapakorn, S., Chrysikopoulos, C.V., 2004. Early breakthrough of colloids and bacteriophage MS2 in a water-saturated sand column. Water Resour. Res. 40 (8) https://doi.org/10.1029/2003WR002676.
Kooi, M., van Nes, E.H., Scheffer, M., Koelmans, A.A., 2017. Ups and downs in the ocean: effects of biofouling on vertical transport of microplastics. Environ. Sci. Technol. 51 (14), 7963–7971. https://doi.org/10.1021/acs.est.6b04702.
Kralova, I., Sjöblom, J., 2009. Surfactants used in food industry: a review. J. Dispers. Sci. Technol. 30 (9), 1363–1383. https://doi.org/10.1080/01932690902735561.
Leij, F.J., Bradford, S.A., 2013. Colloid transport in dual-permeability media. J. Contam. Hydrol. 150, 65–76. https://doi.org/10.1016/j.jconhyd.2013.03.010.
Li, H., Wang, F., Li, J., Deng, S., Zhang, S., 2021. Adsorption of three pesticides on polyethylene microplastics in aqueous solutions: kinetics, isotherms, thermodynamics, and molecular dynamics simulation. Chemosphere 264, 128556. https://doi.org/10.1016/j.chemosphere.2020.128556.
Li, W., Brunetti, G., Zafiu, C., Kunaschk, M., Debreczeby, M., Stumpp, C., 2024. Experimental and simulated microplastics transport in saturated natural sediments: impact of grain size and particle size. J. Hazard. Mater. 133772 https://doi.org/10.1016/j.jhazmat.2024.133772.
Li, X., Scheibe, T.D., Johnson, W.P., 2004. Apparent decreases in colloid deposition rate coefficients with distance of transport under unfavorable deposition conditions: a general phenomenon. Environ. Sci. Technol. 38 (21), 5616–5625. https://doi.org/10.1021/es049154v.
Lin, L., Zuo, L.Z., Peng, J.P., Cai, L.Q., Fok, L., Yan, Y., Li, H.X., Xu, X.R., 2018. Occurrence and distribution of microplastics in an urban river: A case study in the Pearl River along Guangzhou City, China. Sci. Total Environ. 644, 375–381. https://doi.org/10.1016/j.scitotenv.2018.06.327.
Liu, M., Lu, S., Song, Y., Lei, L., Hu, J., Lv, W., Zhou, W., Cao, C., Shi, H., Yang, X., He, D., 2018. Microplastic and mesoplastic pollution in farmland soils in suburbs of Shanghai, China. Environ. Pollut. 242, 855–862. https://doi.org/10.1016/j.envpol.2018.07.051.
Liu, Q., Zhao, B., Santamarina, J.C., 2019. Particle migration and clogging in porous media: a convergent flow microfluidics study. J. Geophys. Res. Solid Earth 124 (9), 9495–9504. https://doi.org/10.1029/2019JB017813.
Lobelle, D., Cunliffe, M., 2011. Early microbial biofilm formation on marine plastic debris. Mar. Pollut. Bull. 62 (1), 197–200. https://doi.org/10.1016/j.marpolbul.2010.10.013.
Logan, B.E., Jewett, D.G., Arnold, R.G., Bouwer, E.J., O'Melia, C.R., 1995. Clarification of clean-bed filtration models. In. J. Environ. Eng. 121 (12), 869–873.
Long, M., Moriceau, B., Gallinari, M., Lambert, C., Huvet, A., Raffray, J., Soudant, P., 2015. Interactions between microplastics and phytoplankton aggregates: impact on their respective fates. Particles in Aquatic Environments: From Invisible Exopolymers to Sinking Aggregates 175, 39–46. https://doi.org/10.1016/j.marchem.2015.04.003.
Lu, X., Wang, X., Liu, X., Singh, V.P., 2023. Dispersal and transport of microplastic particles under different flow conditions in riverine ecosystem. J. Hazard. Mater. 442, 130033 https://doi.org/10.1016/j.jhazmat.2022.130033.
Ma, H., Pazmino, E.F., Johnson, W.P., 2011. Gravitational settling effects on unit cell predictions of colloidal retention in porous Media in the Absence of energy barriers. Environ. Sci. Technol. 45 (19), 8306–8312. https://doi.org/10.1021/es200696x.
Mintenig, S.M., Löder, M.G.J., Primpke, S., Gerdts, G., 2019. Low numbers of microplastics detected in drinking water from ground water sources. Sci. Total Environ. 648, 631–635. https://doi.org/10.1016/j.scitotenv.2018.08.178.
Mistri, M., Infantini, V., Scoponi, M., Granata, T., Moruzzi, L., Massara, F., De Donati, M., Munari, C., 2017. Small plastic debris in sediments from the Central Adriatic Sea: types, occurrence and distribution. Mar. Pollut. Bull. 124 (1), 435–440. https://doi.org/10.1016/j.marpolbul.2017.07.063.
Mu, H., Wang, Y., Zhang, H., Guo, F., Li, A., Zhang, S., Liu, S., Liu, T., 2022. High abundance of microplastics in groundwater in Jiaodong peninsula. China. Sci. Total Environ. 839, 156318 https://doi.org/10.1016/j.scitotenv.2022.156318.
Niehren, S., Kinzelbach, W., 1998. Artificial colloid tracer tests: development of a compact on-line microsphere counter and application to soil column experiments. J. Contam. Hydrol. 35 (1), 249–259. https://doi.org/10.1016/S0169-7722(98)00137-5.
Olkowska, E., Polkowska, Z., Namiesnik, J., 2011. Analytics of surfactants in the environment: problems and challenges. Chem. Rev. 111 (9), 5667–5700.
Park, S., Kim, I., Jeon, W.-H., Moon, H.S., 2023. Exploring the vertical transport of microplastics in subsurface environments: lab-scale experiments and field evidence. J. Contam. Hydrol. 257, 104215 https://doi.org/10.1016/j.jconhyd.2023.104215.
Pazmino, E., Trauscht, J., Johnson, W.P., 2014. Release of colloids from primary minimum contact under unfavorable conditions by perturbations in ionic strength and flow rate. Environ. Sci. Technol. 48 (16), 9227–9235. https://doi.org/10.1021/es502503y.
Ren, Z., Gui, X., Wei, Y., Chen, X., Xu, X., Zhao, L., Qiu, H., Cao, X., 2021. Chemical and photo-initiated aging enhances transport risk of microplastics in saturated soils: key factors, mechanisms, and modeling. Water Res. 202, 117407 https://doi.org/10.1016/j.watres.2021.117407.
Rong, H., Qin, J., He, L., Tong, M., 2023. Cotransport of different electrically charged microplastics with PFOA in saturated porous media. Environ. Pollut. 331, 121862 https://doi.org/10.1016/j.envpol.2023.121862.
Salerno, M.B., Flamm, M., Logan, B.E., Velegol, D., 2006. Transport of rodlike colloids through packed beds. Environ. Sci. Technol. 40 (20), 6336–6340.
Samandra, S., Johnston, J.M., Jaeger, J.E., Symons, B., Xie, S., Currell, M., Ellis, A.V., Clarke, B.O., 2022. Microplastic contamination of an unconfined groundwater aquifer in Victoria. Australia. Sci. Total Environ. 802, 149727 https://doi.org/10.1016/j.scitotenv.2021.149727.
Scheurer, M., Bigalke, M., 2018. Microplastics in Swiss floodplain soils. Environ. Sci. Technol. 52 (6), 3591–3598. https://doi.org/10.1021/acs.est.7b06003.
Schijven, J.F., de Bruin, H.A.M., Hassanizadeh, S.M., de Roda Husman, A.M., 2003. Bacteriophages and clostridium spores as indicator organisms for removal of

pathogens by passage through saturated dune sand. Water Res. 37 (9), 2186–2194. https://doi.org/10.1016/S0043-1354(02)00627-9.
Schwarz, A.E., Ligthart, T.N., Boukris, E., van Harmelen, T., 2019. Sources, transport, and accumulation of different types of plastic litter in aquatic environments: a review study. Mar. Pollut. Bull. 143, 92–100. https://doi.org/10.1016/j.marpolbul.2019.04.029.
Sharma, P., Flury, M., Mattson, E.D., 2008. Studying colloid transport in porous media using a geocentrifuge. Water Resour. Res. 44 (7) https://doi.org/10.1029/2007WR006456.
Shen, C., Li, B., Wang, C., Huang, Y., Jin, Y., 2011. Surface roughness effect on deposition of Nano- and Micro-sized colloids in saturated columns at different solution ionic strengths. Vadose Zone J. 10 (3), 1071–1081. https://doi.org/10.2136/vzj2011.0011.
Sirivithayapakorn, S., Keller, A., 2003. Transport of colloids in saturated porous media: a pore-scale observation of the size exclusion effect and colloid acceleration. Water Resour. Res. 39 (4) https://doi.org/10.1029/2002WR001583.
Soltani, N., Keshavarzi, B., Moore, F., Busquets, R., Nematollahi, M.J., Javid, R., Gobert, S., 2022. Effect of land use on microplastic pollution in a major boundary waterway: the Arvand River. Sci. Total Environ. 830, 154728 https://doi.org/10.1016/j.scitotenv.2022.154728.
Thompson, R.C., Olsen, Y., Mitchell, R.P., Davis, A., Rowland, S.J., John, A.W.G., McGonigle, D., Russell, A.E., 2004. Lost at sea: Where is all the plastic? Science (New York, N.Y.) 304 (5672), 838. https://doi.org/10.1126/science.1094559.
Tong, M., Johnson, W.P., 2006. Excess colloid retention in porous media as a function of colloid size, fluid velocity, and grain angularity. Environ. Sci. Technol. 40 (24), 7725–7731. https://doi.org/10.1021/es061201r.
Torkzaban, S., Bradford, S.A., van Genuchten, M.Th., Walker, S.L., 2008. Colloid transport in unsaturated porous media: the role of water content and ionic strength on particle straining. J. Contam. Hydrol. 96 (1), 113–127. https://doi.org/10.1016/j.jconhyd.2007.10.006.
Tufenkji, N., Elimelech, M., 2004. Deviation from the classical colloid filtration theory in the presence of repulsive DLVO interactions. Langmuir 20 (25), 10818–10828. https://doi.org/10.1021/la0486638.
Waldschläger, K., Schüttrumpf, H., 2020. Infiltration behavior of microplastic particles with different densities, sizes, and shapes—from glass spheres to natural sediments. Environ. Sci. Technol. 54 (15), 9366–9373. https://doi.org/10.1021/acs.est.0c01722.
Wang, H., Lacroix, M., Masséi, N., Dupont, J.-P., 2000. Transport des particules en milieu poreux: Détermination des paramètres hydrodispersifs et du coefficient de dépôt. Comp. Rend. Acad. Sci. Series IIA-Earth Planet. Sci. 331 (2), 97–104. https://doi.org/10.1016/S1251-8050(00)01388-4.
Wang, J., Peng, J., Tan, Z., Gao, Y., Zhan, Z., Chen, Q., Cai, L., 2017. Microplastics in the surface sediments from the Beijiang River littoral zone: composition, abundance, surface textures and interaction with heavy metals. Chemosphere 171, 248–258. https://doi.org/10.1016/j.chemosphere.2016.12.074.
Wang, K., Han, T., Chen, X., Rushimisha, I.E., Liu, Y., Yang, S., Miao, X., Li, X., Weng, L., Li, Y., 2022. Insights into behavior and mechanism of tetracycline adsorption on virgin and soil-exposed microplastics. J. Hazard. Mater. 440, 129770 https://doi.org/10.1016/j.jhazmat.2022.129770.
Weber, C.J., Opp, C., 2020. Spatial patterns of mesoplastics and coarse microplastics in floodplain soils as resulting from land use and fluvial processes. Environ. Pollut. 267, 115390 https://doi.org/10.1016/j.envpol.2020.115390.
Xing, Y., Chen, X., Wagner, R.E., Zhuang, J., Chen, X., 2020. Coupled effect of colloids and surface chemical heterogeneity on the transport of antibiotics in porous media. Sci. Total Environ. 713, 136644 https://doi.org/10.1016/j.scitotenv.2020.136644.
Yang, L., Zhang, Y., Kang, S., Wang, Z., Wu, C., 2021. Microplastics in freshwater sediment: a review on methods, occurrence, and sources. Sci. Total Environ. 754, 141948 https://doi.org/10.1016/j.scitotenv.2020.141948.
Ye, S., Andrady, A.L., 1991. Fouling of floating plastic debris under Biscayne Bay exposure conditions. Mar. Pollut. Bull. 22 (12), 608–613. https://doi.org/10.1016/0025-326X(91)90249-R.
Yiantsios, S.G., Karabelas, A.J., 1998. The effect of gravity on the deposition of micron-sized particles on smooth surfaces. Int. J. Multiphase Flow 24 (2), 283–293. https://doi.org/10.1016/S0301-9322(97)00062-1.
Yiantsios, S.G., Karabelas, A.J., 2003. Deposition of micron-sized particles on flat surfaces: effects of hydrodynamic and physicochemical conditions on particle attachment efficiency. Chem. Eng. Sci. 58 (14), 3105–3113. https://doi.org/10.1016/S0009-2509(03)00169-6.
Yu, Y., Flury, M., 2021. How to take representative samples to quantify microplastic particles in soil? Sci. Total Environ. 784, 147166 https://doi.org/10.1016/j.scitotenv.2021.147166.
Zhang, M., Hou, J., Wu, J., Miao, L., Zeng, Y., 2023. Effects of input concentration, media particle size, and flow rate on fate of polystyrene nanoplastics in saturated porous media. Sci. Total Environ. 881, 163237 https://doi.org/10.1016/j.scitotenv.2023.163237.
Zhao, W., Su, Z., Geng, T., Zhao, Y., Tian, Y., Zhao, P., 2022a. Effects of ionic strength and particle size on transport of microplastic and humic acid in porous media. Chemosphere 309, 136593. https://doi.org/10.1016/j.chemosphere.2022.136593.
Zhao, Z., Zhao, K., Zhang, T., Xu, Y., Chen, R., Xue, S., Liu, M., Tang, D., Yang, X., Giessen, V., 2022b. Irrigation-facilitated low-density polyethylene microplastic vertical transport along soil profile: an empirical model developed by column experiment. Ecotoxicol. Environ. Saf. 247, 114232 https://doi.org/10.1016/j.ecoenv.2022.114232.